Reading:
J. H. Gross: Mass Spectrometry (A Textbook, Springer)
L. Sleno and D. A. Volmer, *J. Mass Spectrom.* **2004**, *39*, 1091.
J. S. Brodbelt, *Anal. Chem.* **2016**, *88*, 30.

Tandem MS techniques

Structure elucidation by MS connected with soft ionization techniques, bond dissociation energies

EI vs. soft ionization techniques

$C_6H_{12}O_6$

M = 180 g/mol

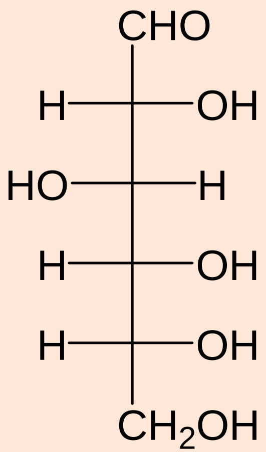

EI

→ Lot of "structural" information

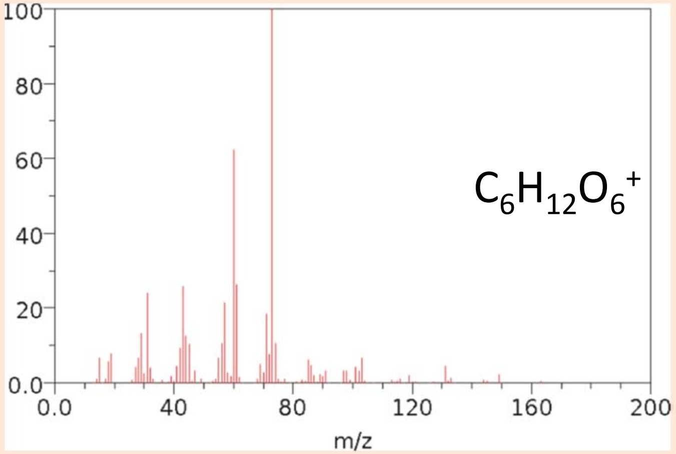

CI, ESI, MALDI

→ m/z ratio

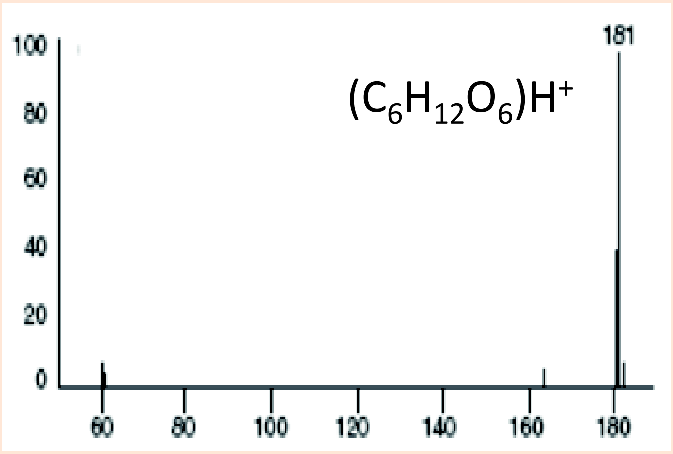

→ For structural information, we need to induce fragmentation

Tandem MS

- Looking at products of unimolecular or bimolecular reactions of mass-selected ions
- Necessity of at least two mass-filtering events (MS/MS)
- Typical instruments:
  - Ion traps
  - Triple quadrupoles (typically quadrupole-octopole-quadrupole arrangement)
  - Q-TOF

Tandem in Space vs. Tandem in Time

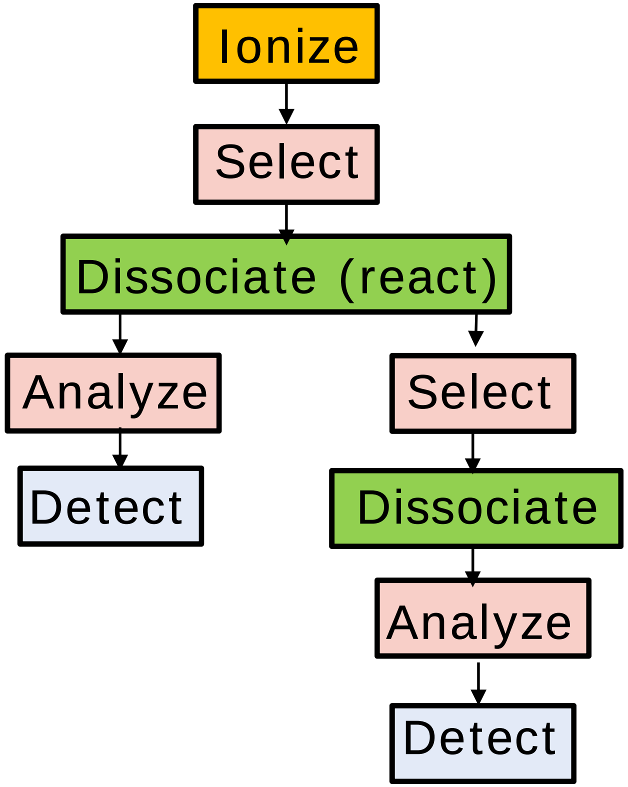

Ionize
Select
Dissociate (react)
Analyze
Detect
Select
Dissociate
Analyze
Detect

Beam transmitting devices:
Multiple sector instruments,
TOF/TOF, QqQ, QhQ, QoQ,
QqTOF

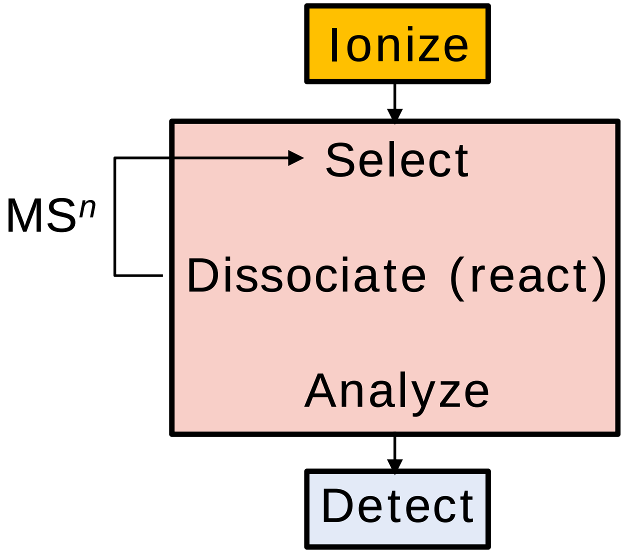

Ionize
MS^n
Select
Dissociate (react)
Analyze
Detect

Single m/z analyzer in a pulsed regime:
Quadrupole ion traps
FT-ICR

Collision induced dissociation (CID)

- Tandem in space: ion beam passes through a collision cell with an inert collision gas (He, N_2, Ar, Xe)

- Fragmentation depends on the collision energy and the collision gas pressure

- Energy transfer during collisions $AB^+ + N \rightarrow [AB^+]^* + N \rightarrow A^+ + B + N$

$$E_{CM} = E_{LAB}\,\frac{m_N}{m_N + m_{AB}}$$

- In high collision energy regime (TOF, sectors)
He - still large energy transfer
- “no” charge transfer

- In low collision energy regime (q)
N_2, Ar, Xe

Pressure measurements!

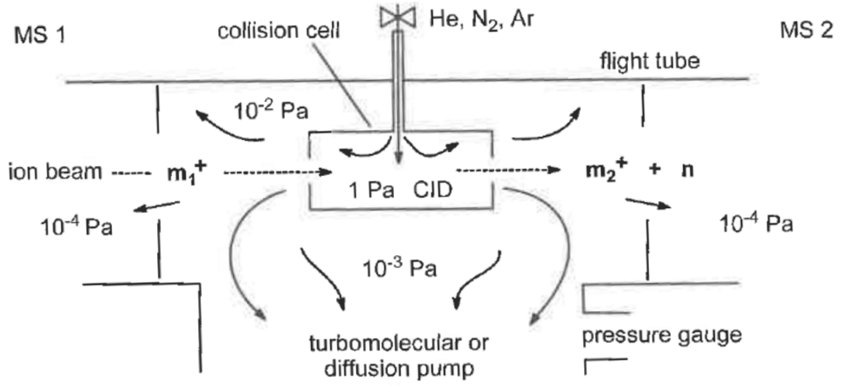

Fig. 9.4. Schematic of a collision cell for CID experiments in a beam instrument. Ions mass-selected in MS1 enter from the left.

Single and Multiple Collisions in CID

- Collision gas pressure can be indirectly adjusted by the attenuation of the beam of mass-selected ions
  - Transmission 90% → 95% of the ions undergo a single collision
    5% - two collisions
  - Transmission 50% → 68% of the ions undergo a single collision
    23% - two collisions, the rest – three and four collisions

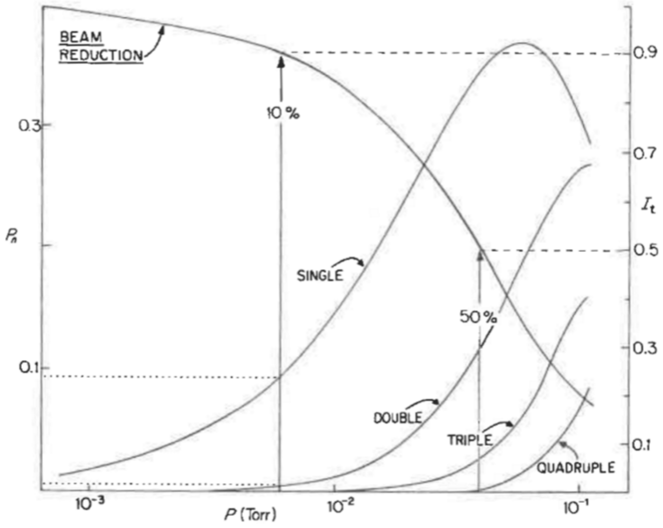

Fig. 9.7. Total collision probability P_n (*left* ordinate) and fractions of single, double, triple, and quadruple collisions vs. collision gas pressure. The transmission of the main beam I_t is given on the *right* ordinate. *Dotted lines* mark beam transmission and collision probabilities for 90% and 50% transmission, respectively. Values are calculated for an ion of collision cross section 5×10^{-16} cm^2 and 1 cm collision path; 10^{-2} Torr = 1.33 Pa. Adapted from Ref. [17] with permission. © John Wiley & Sons, 1985.

- Lambert-Beer law:
  - Beams: $[M_p] = [M_p]_0 \times e^{-n\sigma l}$
    n – gas density
    l – length of the collision cell
    σ – collision cross section
  - Traps: $[M_p] = [M_p]_0 \times e^{-nkt}$
    n – gas density
    k – sum of rate constants for loss of M_p
    t – time

- Optimally: medium transmission

QqQ, QhQ, QoQ

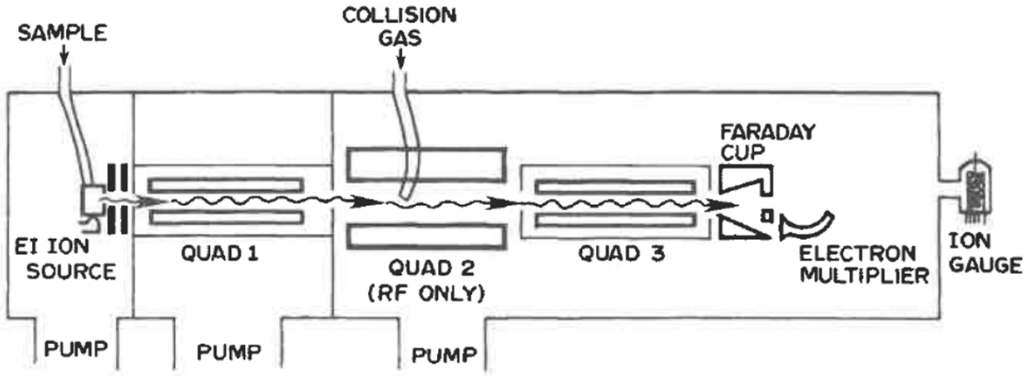

Fig. 9.17. Schematic of an early triple quadrupole mass spectrometer (QqQ). Reproduced from Ref. [90] with permission. © Elsevier Science, 1979.

Product ion scan (CID, collision induced dissociation)

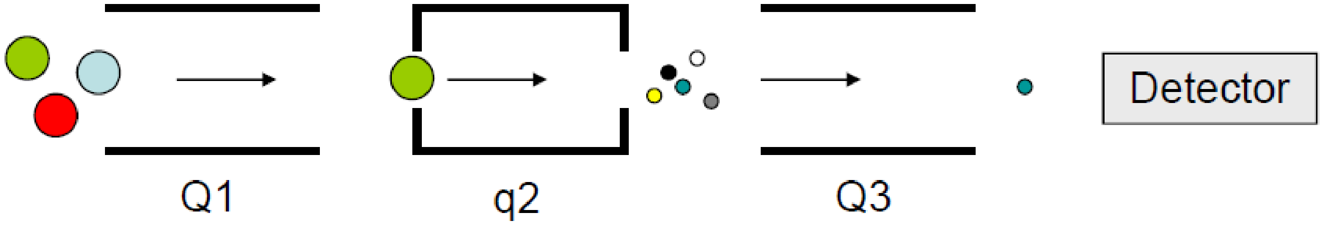

- https://www.youtube.com/watch?v=WHoXZaCqM1g

QqQ, QhQ, QoQ

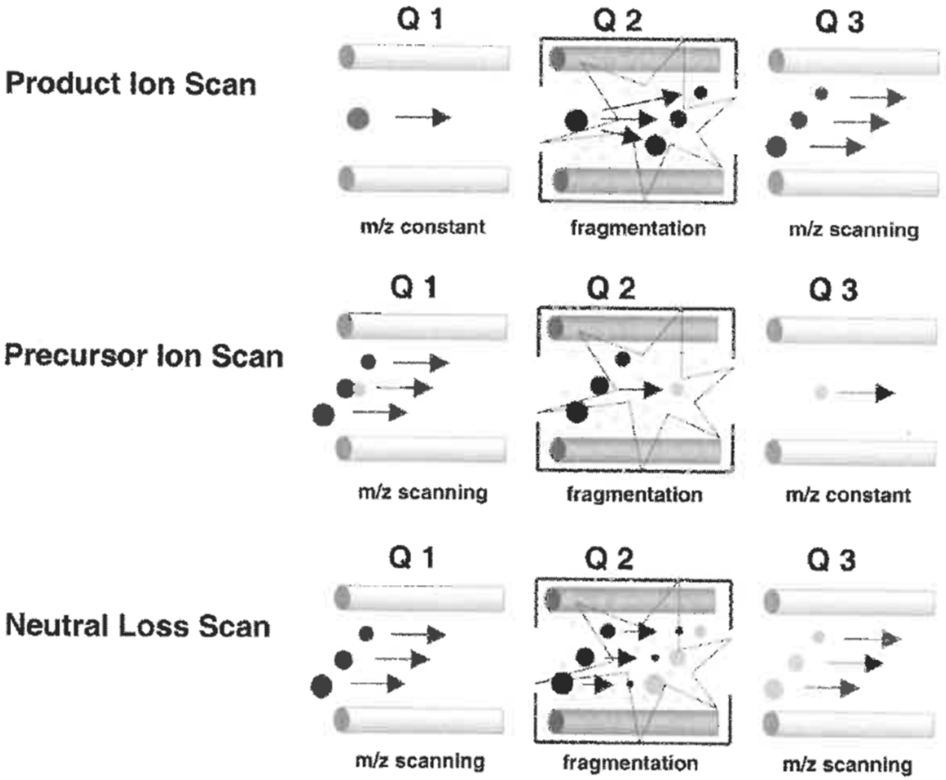

Fig. 9.18. Scan modes of triple quadrupole mass spectrometers. Adapted from Ref. [98] with permission. © Springer-Verlag, 2004.

Applications: Bond Dissociation Energies (*BDE*s)

Cascade cyclisation reactions of polyynes a enynes

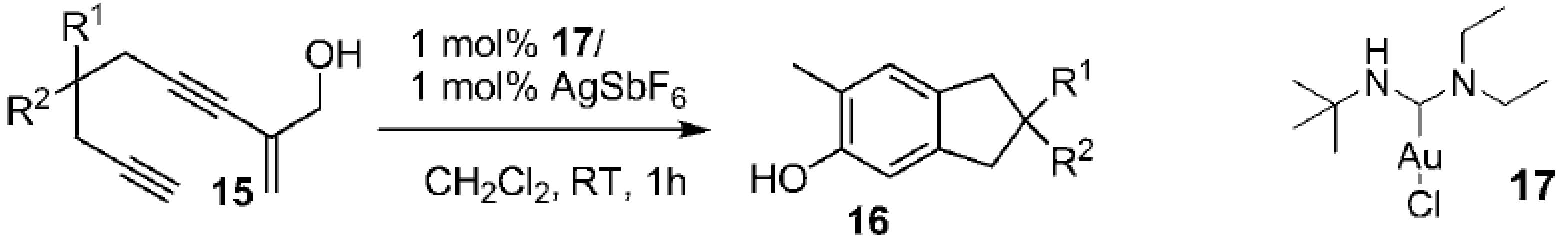

Hashmi, A. S. K. et al. *Chem. Eur. J.* 2011, *17*, 8195.

- What is the first step?
- Where does $[LAu]^+$ coordinates preferentially?

→ Binding energies to different multiple C-C bonds:

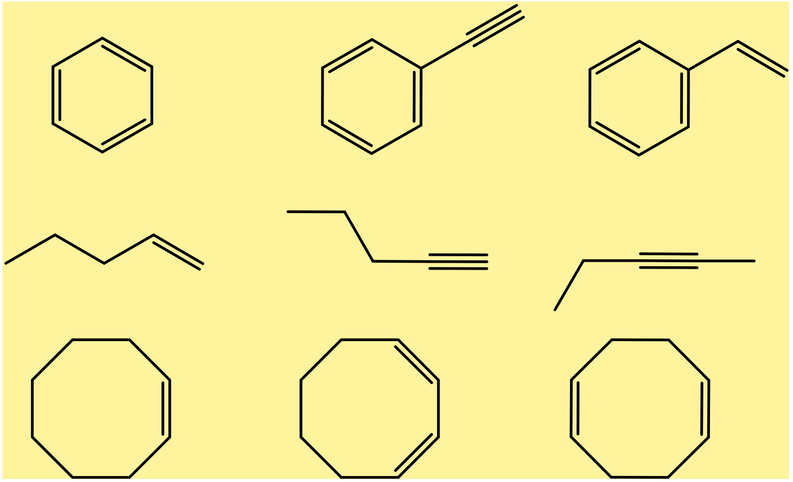

Bond dissociation energies

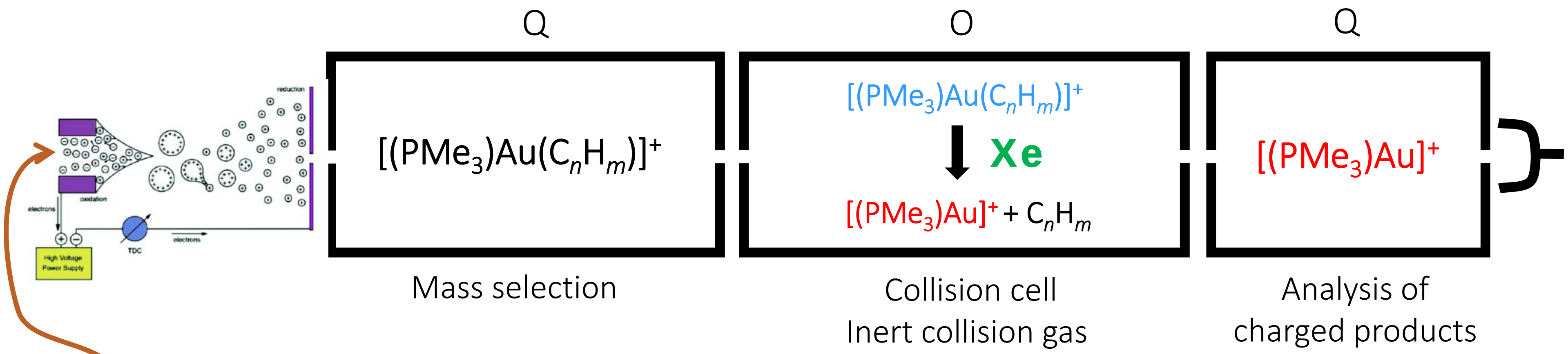

Q

$[(PMe_3)Au(C_nH_m)]^+$

Mass selection

O

$[(PMe_3)Au(C_nH_m)]^+$

Xe

$[(PMe_3)Au]^+ + C_nH_m$

Collision cell
Inert collision gas

Q

$[(PMe_3)Au]^+$

Analysis of
charged products

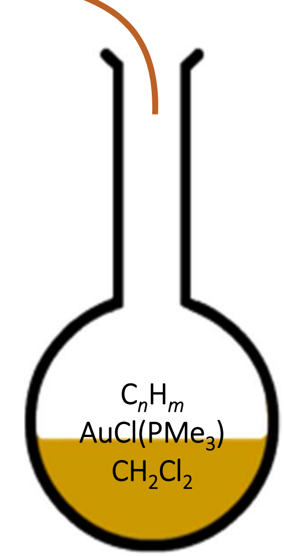

C_nH_m
$AuCl(PMe_3)$
CH_2Cl_2

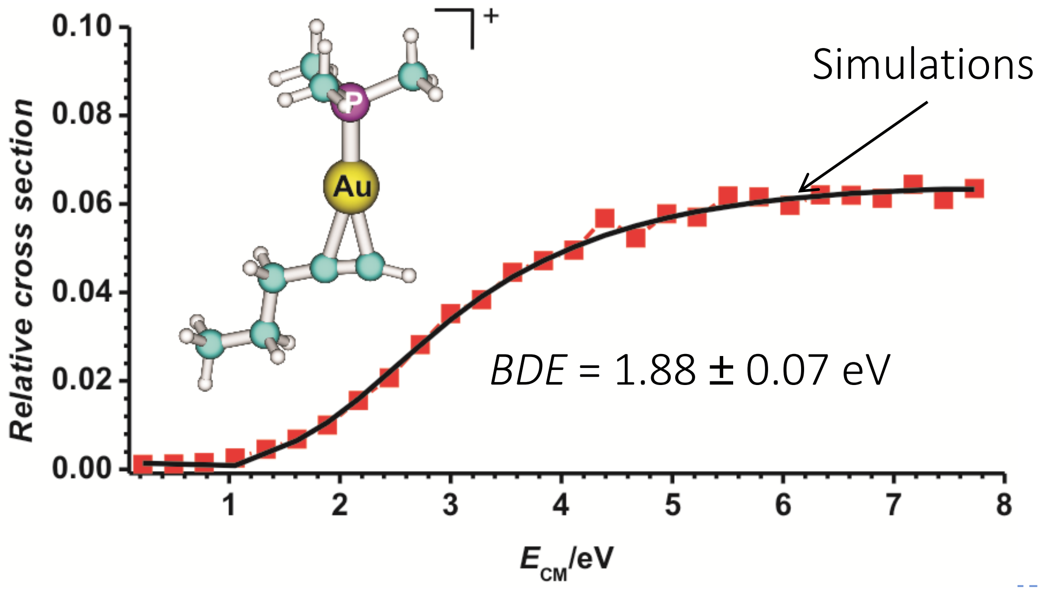

BDE = 1.88 ± 0.07 eV

C_nH_m	BDE_{exp} [eV]
Styren	1.85 ± 0.04
Fenylacetylen	1.87 ± 0.04
Benzen	1.68 ± 0.03
1-Penten	1.82 ± 0.05
1-Pentyn	1.88 ± 0.07
2-Pentyn	1.91 ± 0.04
Cyclookten	1.89 ± 0.02
1,5-Cyclooktadien	1.93 ± 0.03
1,3-Cyclooktadien	1.83 ± 0.03

Organometallics 2012, *31*, 1935.

Unimolecular dissociation

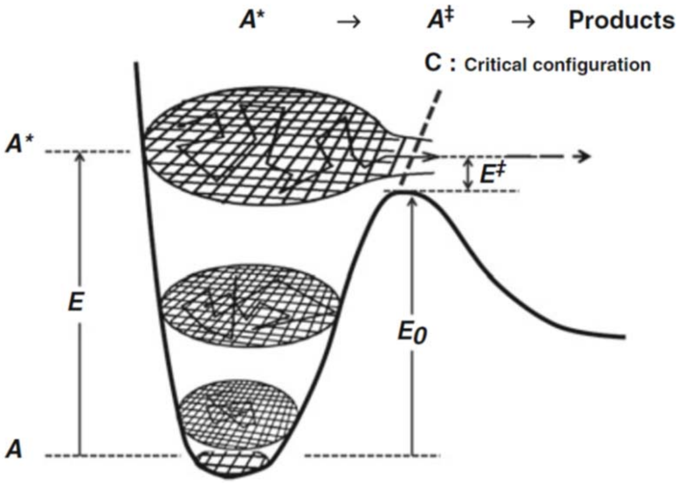

Statistical theory:

$$k(E) = \frac{s}{h}\left[\frac{P^{\neq}(E - E_0)}{\rho_E}\right]$$

h – Planck's constant
s – number of equivalent reaction routes
E – internal energy
E_0 – threshold energy
$P^{\neq}(E - E_0)$ – total number of states of the transition state in the energy span
ρ_E – density of states of the molecule at energy E

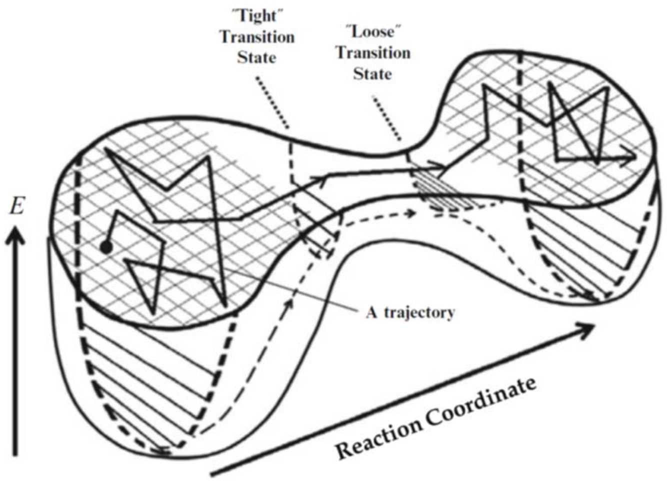

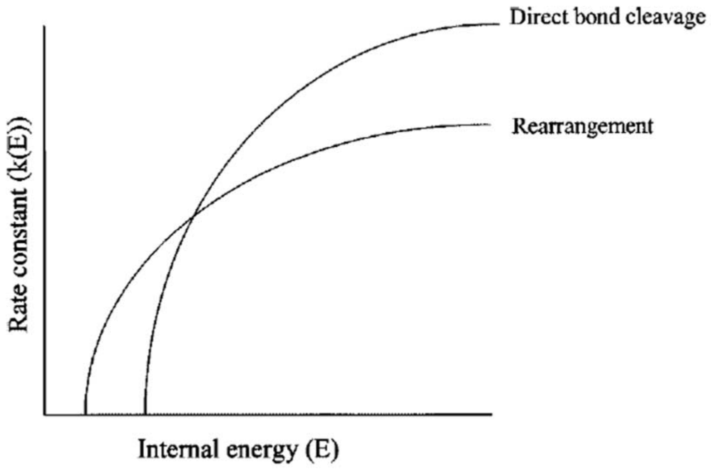

Figure 2. Arbitrary internal energy curves for rearrangement and simple bond cleavage fragmentation reactions.

T. Nishimura, Fundamentals of Mass Spectrometry, K. Hiraoka (ed.), Springer Science.

Unimolecular dissociation

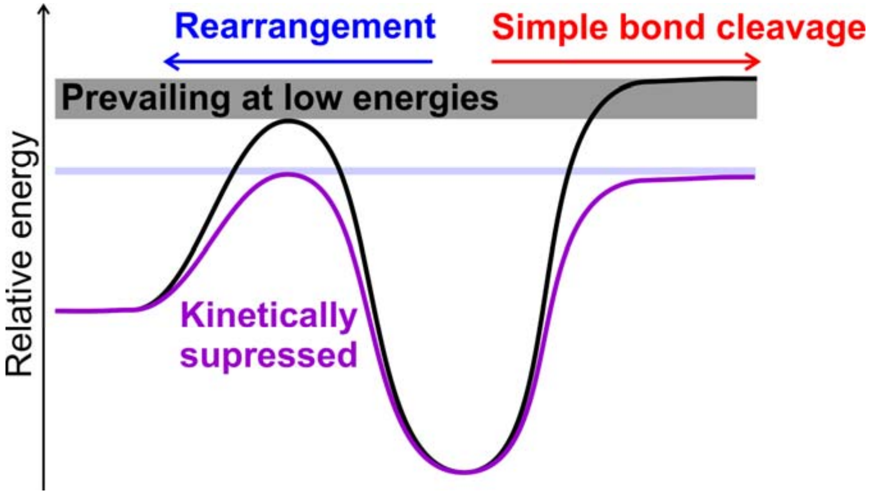

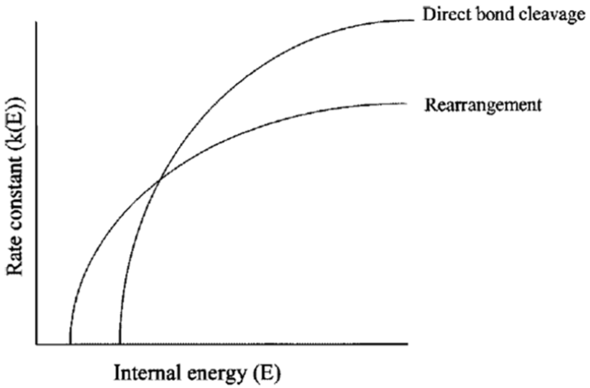

Figure 2. Arbitrary internal energy curves for rearrangement and simple bond cleavage fragmentation reactions.

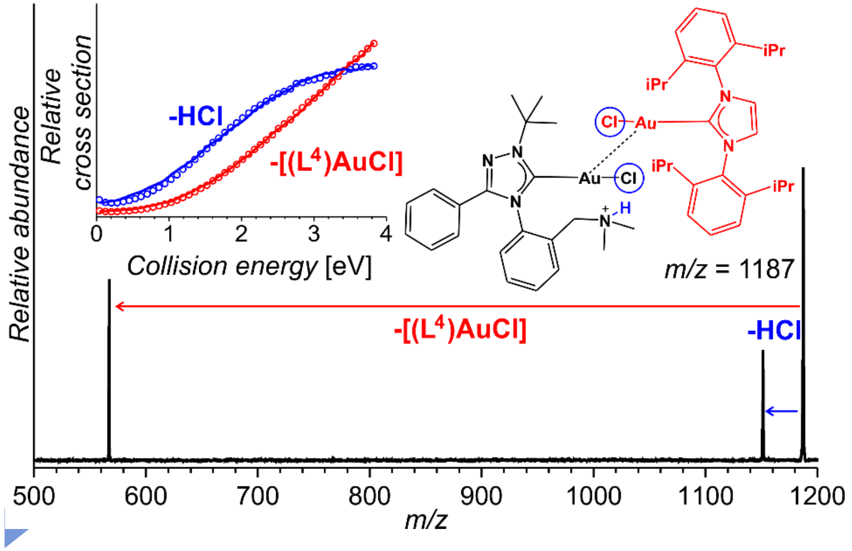

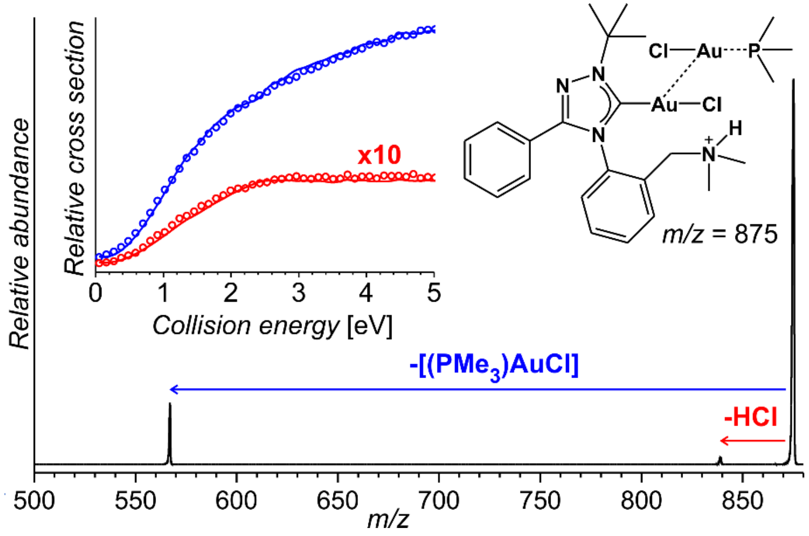

E. Andris et al., *J. Am. Chem. Soc.* **2018**, 140, 2316

Bond dissociation energies

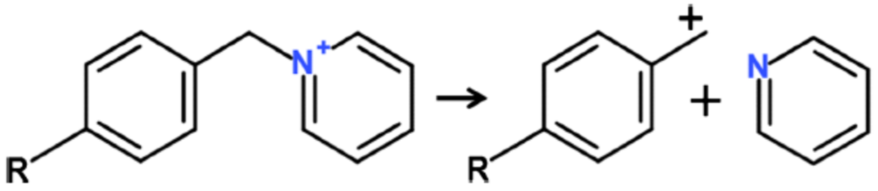

(thermometer ions)

Table 2. Comparison of Experimental and Theoretical Bond Dissociation Energies (eV) for Dissociation of RBn

R	Product ion	Exp[a]	B3LYP-GD3BJ[a]	M06-GD3[a]	MP2(full)[a]	AM1[b]	HF[c]
p-OCH_3	RBn^+	1.93 ± 0.08	1.63 (1.66)	1.67 (1.71)	1.86 (2.14)	1.3	1.4
p-CH_3	RBn^+	2.26 ± 0.13	1.99 (2.02)	2.01 (2.05)	2.26 (2.54)	1.6	1.8
H	RBn^+	2.58 ± 0.15	2.25 (2.28)	2.27 (2.31)	2.48 (2.75)		
p-NO_2	RBn^+	3.04 ± 0.12	2.62 (2.65)	2.66 (2.71)	2.79 (3.06)	2.1	
MAD[g]		0.12[h]	0.33 ± 0.07 (0.30 ±0.07)	0.30 ± 0.06 (0.26 ± 0.06)	0.11 ± 0.11 (0.17 ± 0.11)	0.75 ± 0.18	0.5
p-NO_2	$BnPy^+$	2.68 ± 0.13	2.72 (2.77)	2.77 (2.86)	2.65 (2.93)		
p-NO_2	$TS(O_2NBn^+)$	4.56 ± 0.12	4.13 (4.16)	4.03 (4.08)	4.34 (4.61)		

[a] This work. All values calculated at the level of theory indicated using a 6-311+G(2d,2p) basis set. Geometry op
0.989) for zero-point energy corrections are calculated at the B3LYP/6-311+G(d,p) level of theory. Values exclu

[b] Reference [53].

[c] 6-31G(d) basis set. Reference [9].

[d] 6-31G basis set. Reference [9].

[e] 6-31+G(d) basis set. References [10] and [11].

[f] CCSD(T)/6-311++G(d,p)//B3LYP/6-311++G(2d,p). Reference [8].

[g] Mean absolute deviations from experiment.

[h] Mean experimental uncertainty.

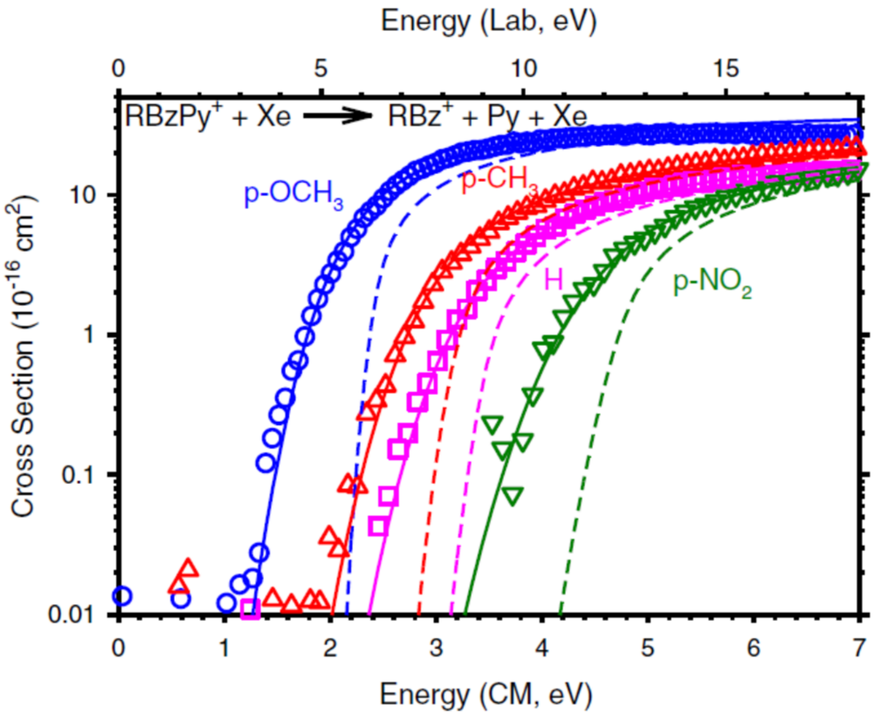

Figure 2. Zero-pressure extrapolated CID cross-sections for reaction 1 of the four benzylpyridinium cations studied (R = p-OCH_3, p-CH_3, H, p-NO_2) as a function of the kinetic energy in the center-of-mass frame (lower x-axis) and laboratory frame for R = p-OCH_3 (upper x-axis). Solid lines represent the model of Equation 2 convoluted with the internal and kinetic energy distributions of the reactants. Dashed lines represent the model cross-sections in the absence of kinetic energy broadening for reactants having an internal energy of 0 K

- J. E. Carpenter et al., *J. Am. Soc. Mass Spectrom.* **2017**, *28*, 1876 (Armentrout)

Bond dissociation energies

- Programs for simulations
  - Crunch (Armentrout)
  - L-CID (Chen)

- What to take care about
  - Models consider only single-collision events (extrapolation to zero pressure)
  - Care about initial distribution of kinetic energy
  - Classical QqQ, QhQ, QoQ only
  - 2 fragmention channels only

Kinetic method

Interested in basicity?

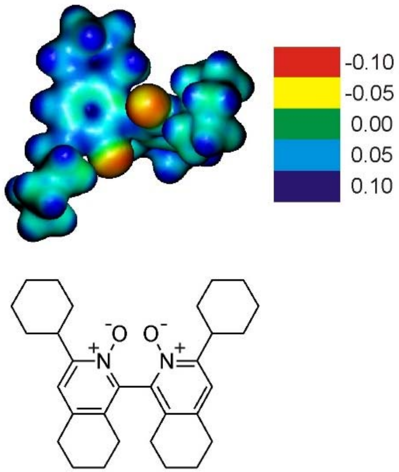

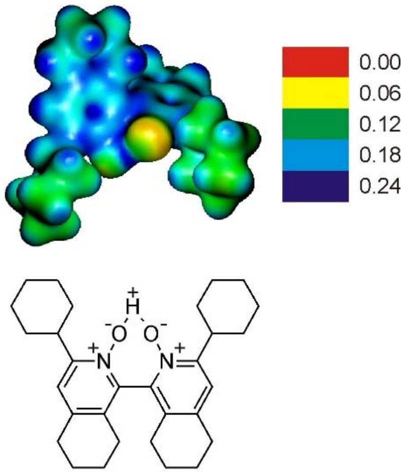

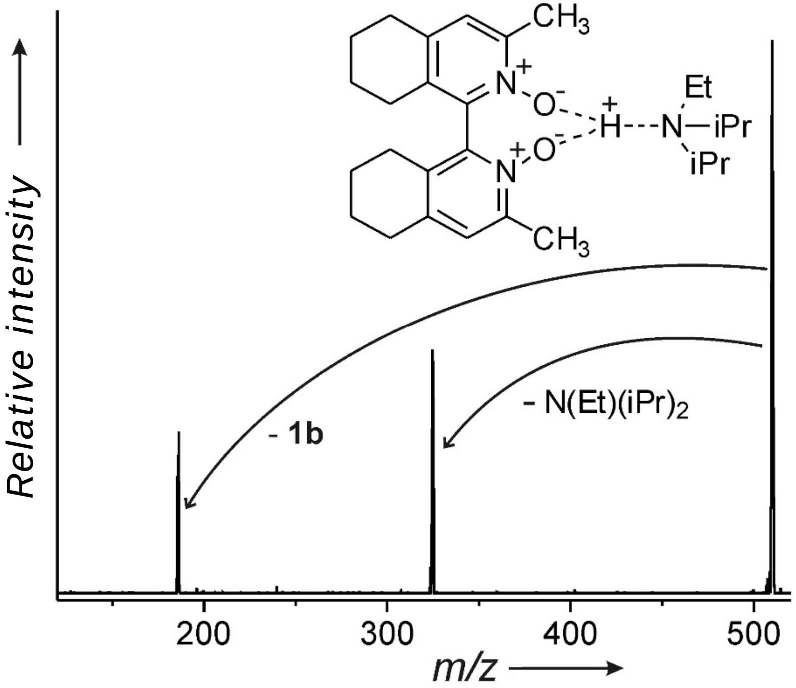

$$\ln\left(\frac{I_{AH^+}}{I_{BH^+}}\right) \approx \ln\left(\frac{k_A}{k_B}\right) \approx \frac{\Delta G_A - \Delta G_B}{RT_{eff}} \approx \frac{GB_A - GB_B}{RT_{eff}} \approx \frac{PA_A - PA_B}{RT_{eff}}$$

- Read for the next tutorial: R. G. Cooks, P. Sh. H. Wong, Acc. Chem. Res. 1998, 31, 379.
  L. Duchackova et al., J. Am. Chem. Soc. 2010, 132, 12660.

Quadrupole ion traps

$$q_z = \frac{8ezV}{m(r_0^2 + 2z_0^2)(2\pi\upsilon)^2}$$

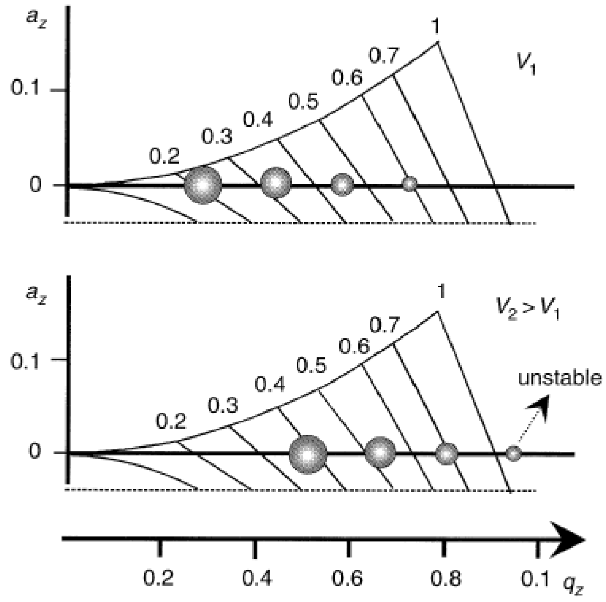

Figure 2.20
At a fixed value of the RF potential V applied to the ring electrode, heavier ions will have lower β_z values and thus lower secular frequencies. If V is increased, β_z values increase for all the ions, as do the secular frequencies. In the example given, the lightest ion now has a β_z value larger than unity and is thus expelled from the trap. The highest mass that can be analyzed depends on the limit V value that can be applied: around 7000–8000 V from zero to peak. For a trap having $r_0 = 1$ cm and operating at a ν frequency of 1.1 MHz, the highest detectable mass-to-charge ratio is about 650 Th

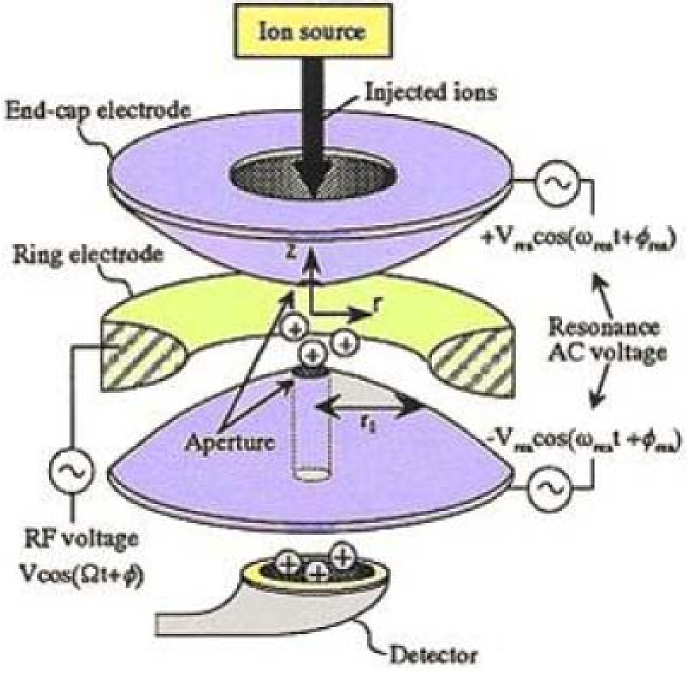

Secular frequency

- Ions oscillate at secular frequency *f* that is smaller than ν
- Along *z* axis, f_z is proportional to q_z
- If RF with frequency f_z is applied to the end-cap electrodes, ions with secular frequency f_z will be in resonance and amplitude of their oscillation along the z axis will increase → for sufficiently large amplitudes are ions expelled

$$q_Z = \frac{8ezV}{m(r_0^2 + 2z_0^2)(2\pi\upsilon)^2}$$

Example:

ν=1,1 MHz induces oscillations of ions with a given m/z with frequency f_z = 160 kHz

End-cap electrodes: RF with *f´* = 160 kHz

→ Resonant energy transfer will destabilize ions along the z axis

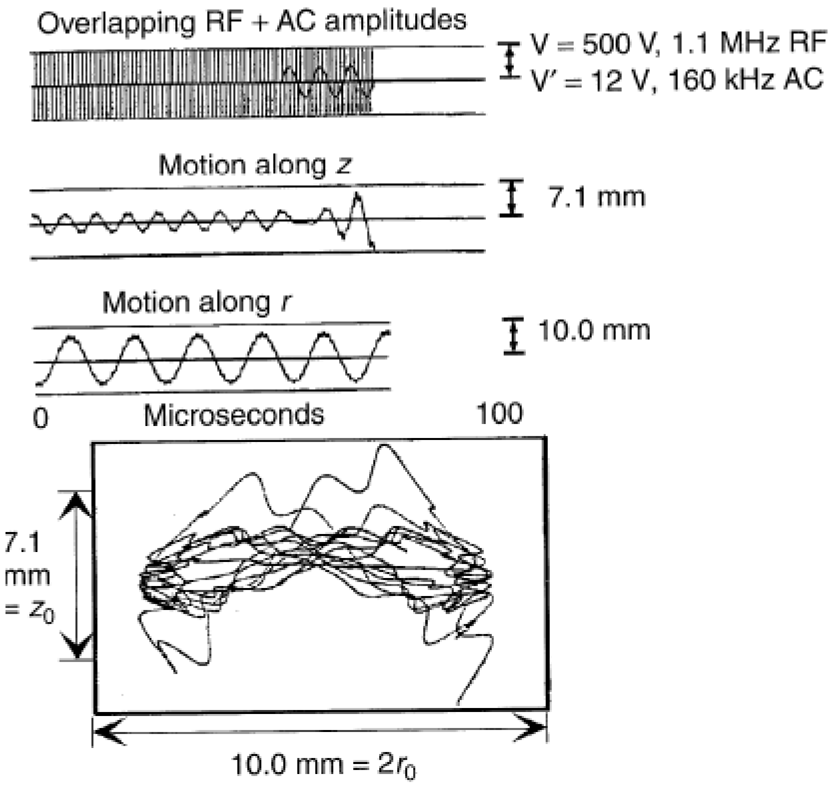

From de Hoffmann

Mass selection

- Apply AC field to the end cap electrodes
  → point of instability (for given f_z)
- Scan amplitude of fundamental RF
  - Scan downwards → ejection of all heavier ions
  - Scan upwards → ejection of all lighter ions

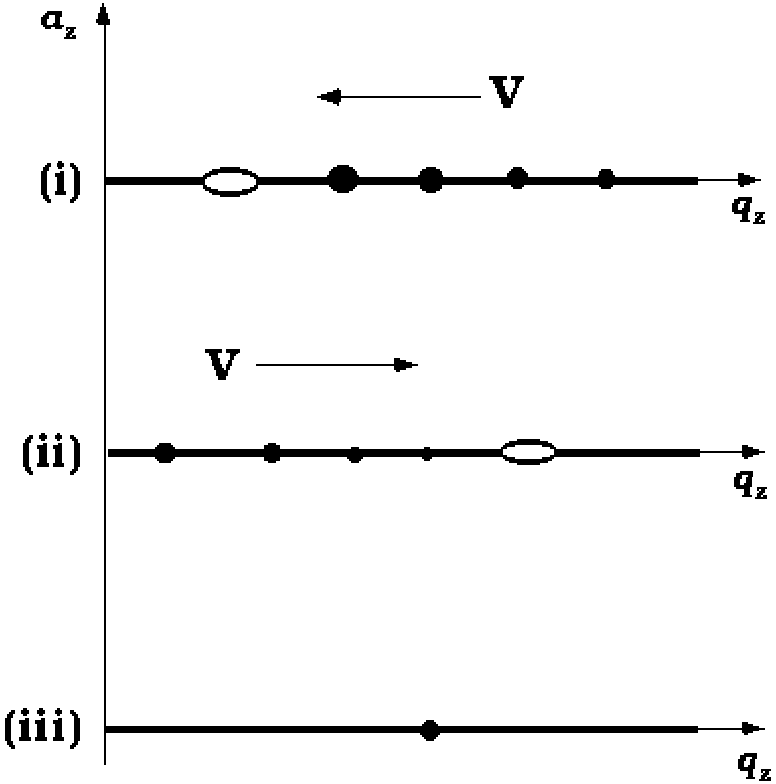

$$q_Z = \frac{8ezV}{m(r_0^2 + 2z_0^2)(2\pi\upsilon)^2}$$

MS/MS

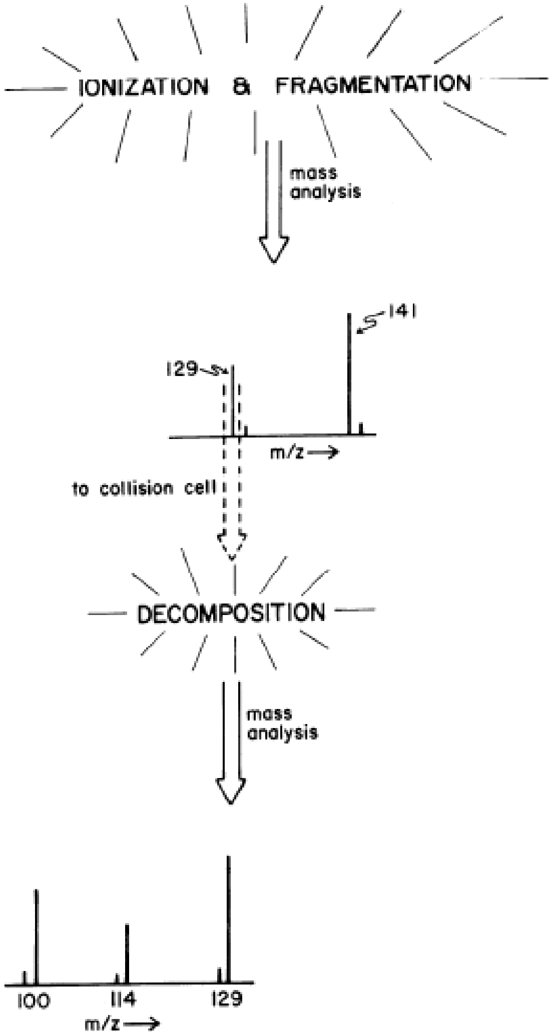

FIG. 5.1. Conceptual representation of the technique of MS/MS. In this case, ions of *m/z* 129 are selected by the first mass spectrometer; these ions are directed into a collision chamber, and the decomposition products are analyzed by the second mass spectrometer to produce the product-ion spectrum of *m/z* 129 **(bottom)**.

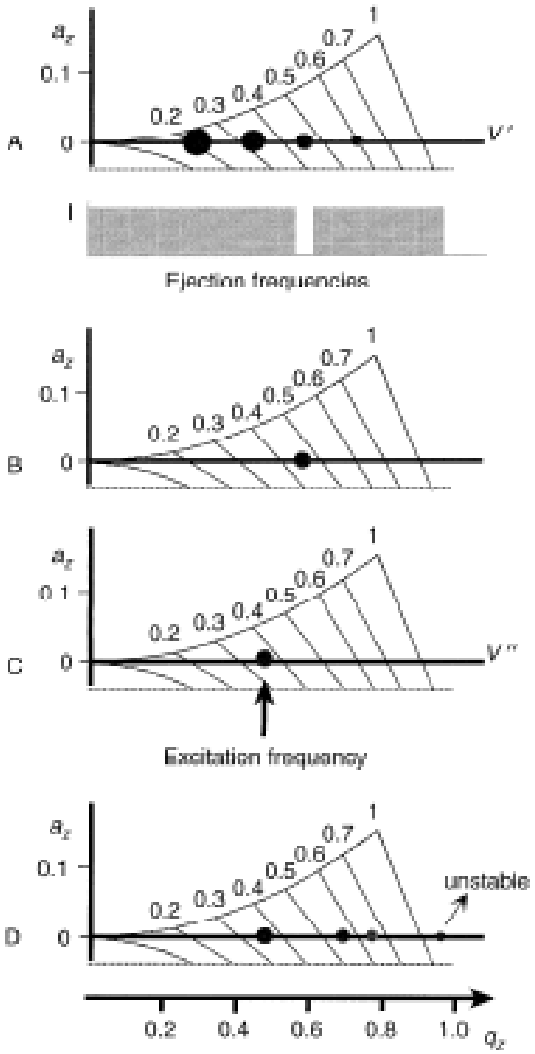

Figure 2.25
One possible sequence of events to produce an MS/MS spectrum. (A) Ions of one mass-to-charge ratio are selected by expelling all the others at their resonance frequency applied to the caps. (B) Only ions of the selected *m/z* are present in the trap. (C) Voltage *V* is adjusted so as to bring the ion in resonance with the excitation frequency applied to the caps. (D) Ions are analyzed by ejection at the stability limit

Applications - *BDEs*

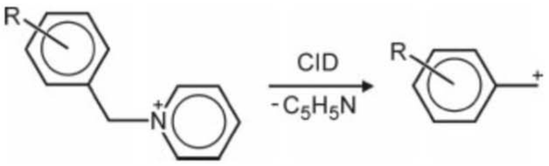

Scheme 1. Generation of benzylium ions upon CID of benzylpyridinium ions concomitant with the loss of neutral pyridine.

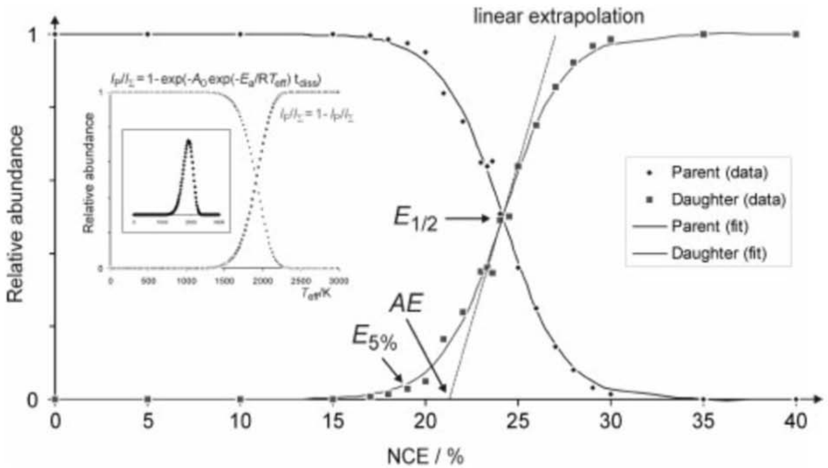

Figure 1. Breakdown diagram of mass-selected $[p\text{-}FC_6H_4\text{-}CH_2\text{-}NC_5H_5]^+$ as a function of the relative collision energy. The dots are the experimental data; the solid lines are the sigmoid functions used for analysis. To assist understanding of the text, the parameters representing the threshold behavior ($E_{5\%}$, AE and $E_{1/2}$) are indicated in the figure. For the description of the inset, see text.

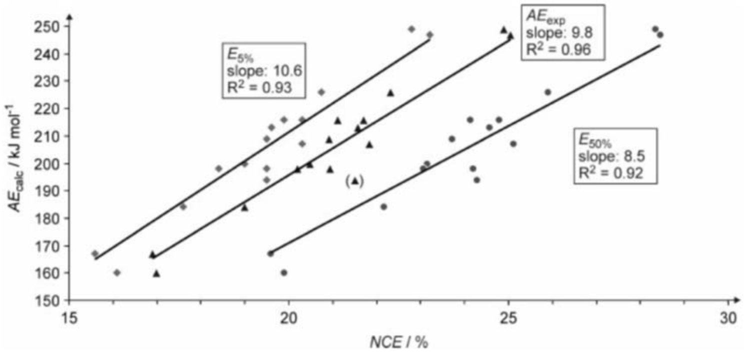

Figure 2. Plot of the characteristic experimental parameters $E_{5\%}$, $E_{50\%}$ and AE_{exp} *versus* the computed values AE_{calc} and the resulting linear equations and correlation coefficients. Note that all correlations are forced to cross the origin. In the correlation of AE *versus* NCE, the point for R = *t*-Bu (triangle in brackets) is not included (see below).

- E. L. Zins, C. Pepe, D. Schröder, *J. Mass Spectrom.* **2010**, *45*, 1253.

Applications - *BDEs*

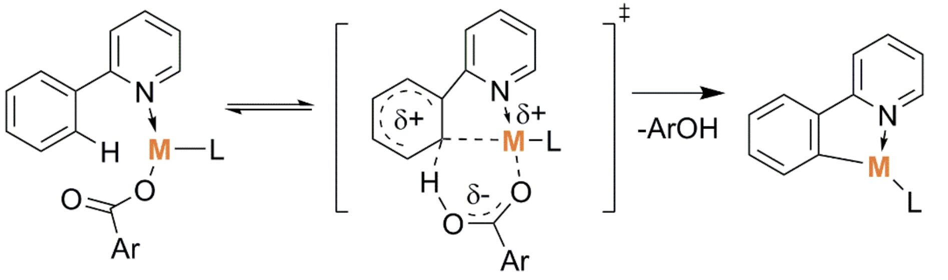

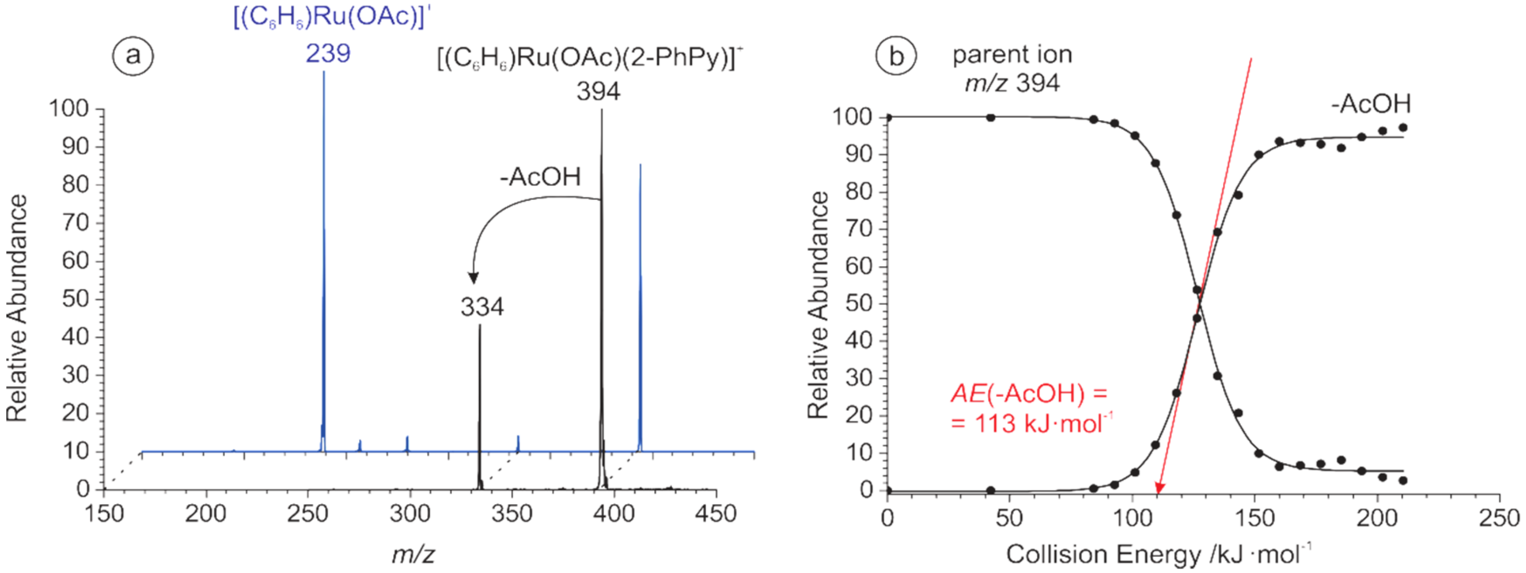

a) CID spectra of the mass selected peak at *m/z* 394 for 2-PhPy (black) and 3-PhPy (blue);
b) the breakdown curve for *m/z* 394 (2-PhPy). The appearance energy for acetic acid loss was determined to be *AE*(-AcOH) = 113 ± 3 kJ·mol^{-1}.

Structure elucidation: Proteins

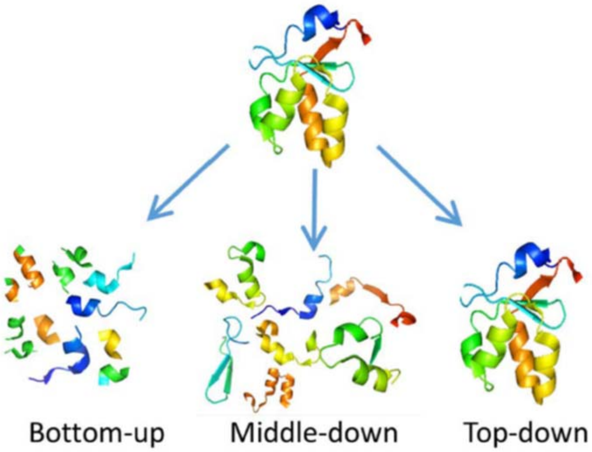

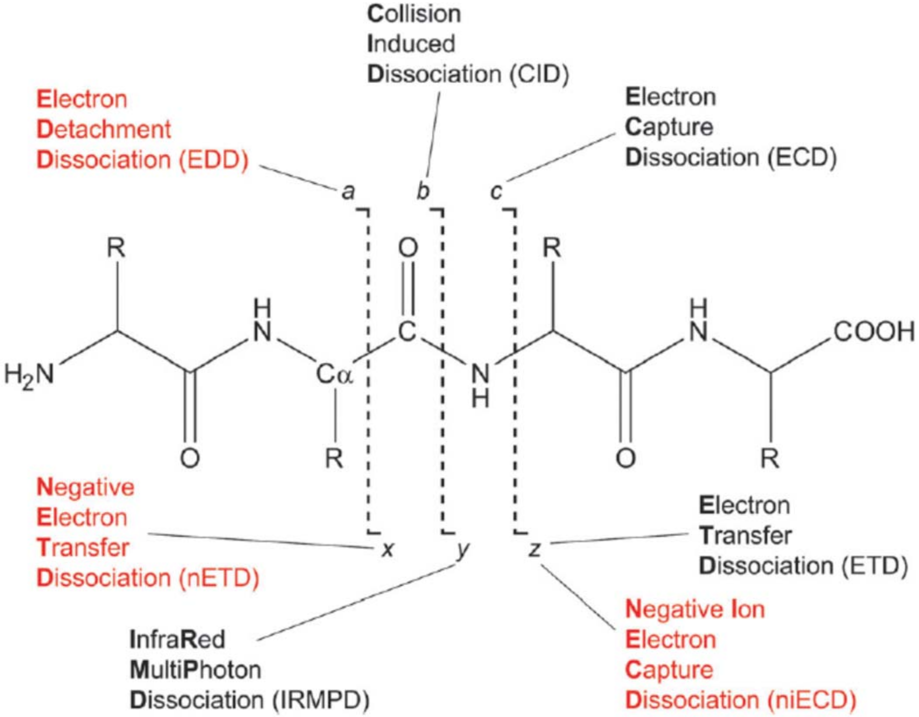

Fig. 1 Peptide backbone fragmentation: peptide structure, selected tandem mass spectrometric (MS/MS) techniques, and fragment ion nomenclature. Electron-mediated techniques for anionic analytes are highlighted in red.

Fragmentation in ICR

- CID (collision induced dissociation)
  - Similarly as in the ion traps – selective for a given m/z
    Resonance excitation (0.1 – 0.5 ms)
    SORI: sustained off resonance irradiation (0.1 – 1 s, E_{coll} < 10 eV)
- IRMPD
- ETD

SORI:

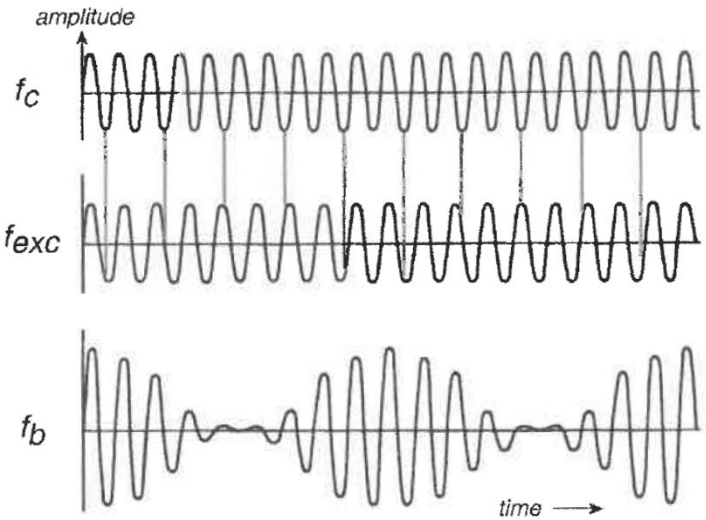

Infrared multiphoton dissociation

- Ions have to be isolated (ICR, quadrupole ion traps)

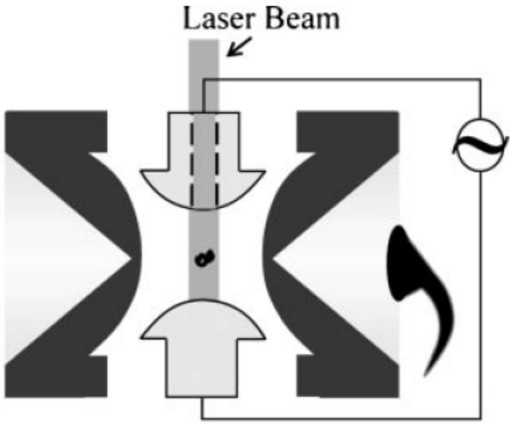

- Dissociation induced by absorption of many IR photons

  1 IR photon ~ 3 kcal/mol

  bonding energies ~ 50 kcal/mol

- Quasi-continuum of vibrational states for a given range of photon energies – at least one suitable vibrational transition

- First experiments:

  $[(C_2H_5)_2O]_2H^+ \rightarrow (C_2H_5)_2OH^+ + (C_2H_5)_2O$

  - IR absorption induces the cluster fragmentation
  - Density of states of the cluster after absorption of one photon ~ kvazikontinuum

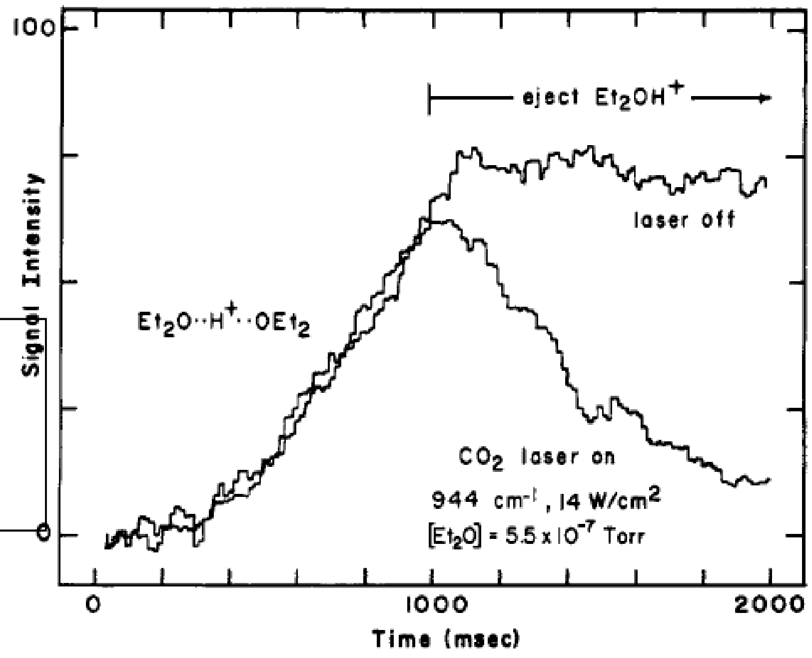

R. L. Woodin, D. S. Bomse, J. L. Beauchamp, *J. Am. Chem. Soc.* **1978**, *100*, 3248;
D. S. Bomse, R. L. Woodin, and J. L. Beauchamp, *J. Am. Chem. Soc.* **1979**, *101*, 5503.

IRMPD

- Large molecules – ideal for – quasicontinuum of vibrational states achieved at the laboratory temperature
- Usually **CO_2 lasers**
- Quadrupole ion traps

  IR absorption (heating) vs. collisional cooling of internal energy

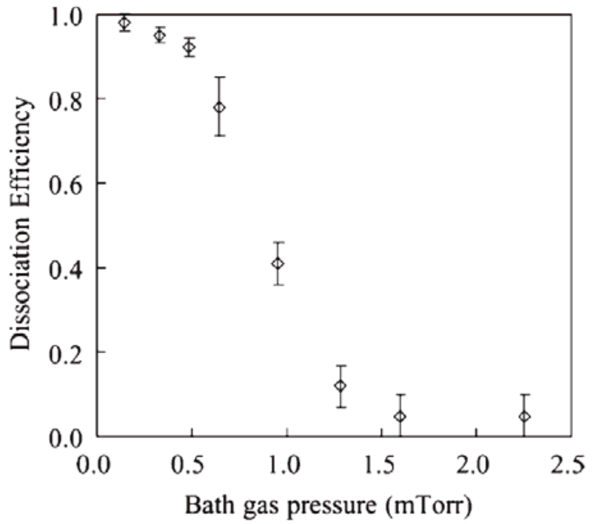

Comparison of CID and IRMPD

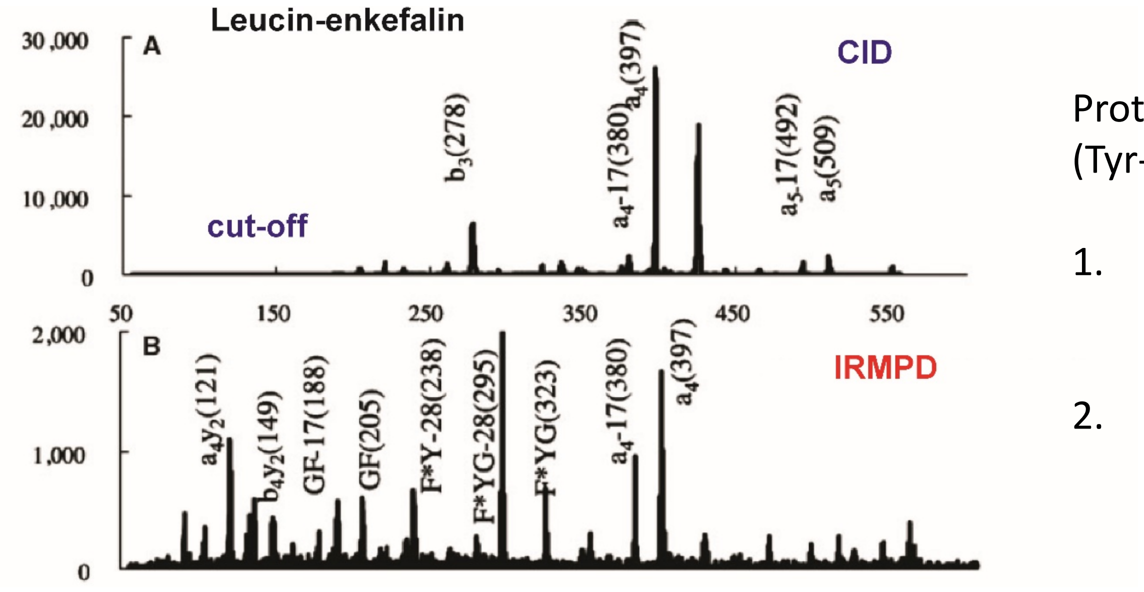

Protonated peptide Leucin-enkefaline (Tyr-Gly-Gly-Phe-Leu)

1. In IRMPD spectra - also fragments with low masses
2. Fragments can also absorb IR photons and further fragment → fragmentations more extensive

Y. Hashimoto, H. Hasegawa, I. Waki, *Rapid Commun. Mass Spectrom.* **2004**, *18*, 2255.

Electron Capture Dissociation (ECD)

- EC increases with the square of the ionic charge → multiply charged ions are ideal targets
- Energy of electrons < 0.2 eV (carefully heated filament)
- Ions have to be trapped (FT-ICR only)
- EC leads to ions with reduced charge and higher internal energy → dissociation
- Capture of electron changes even e- ion to odd e- ion → alternative fragmentation channels to CID or IRMPD

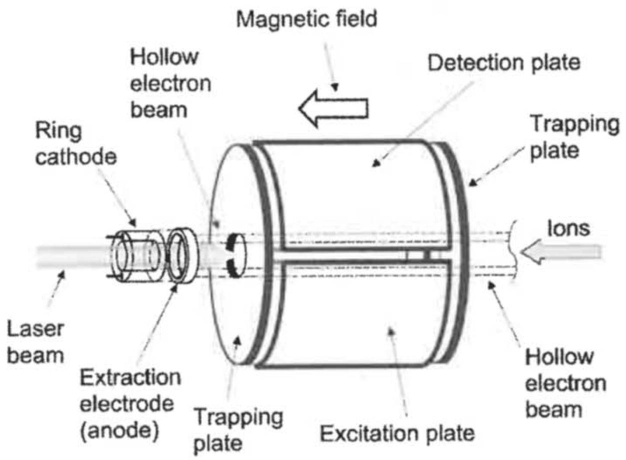

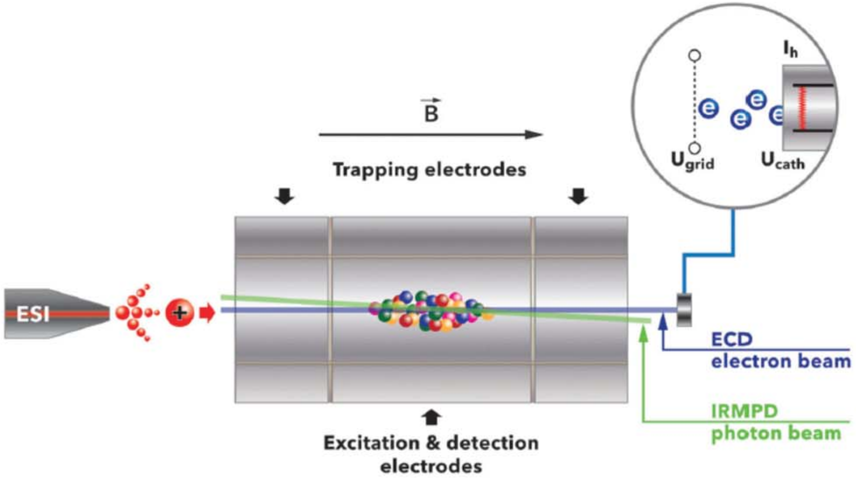

Fig. 9.36. Combined ECD and IRMPD setup for FT-ICR-MS. Reproduced from Ref. [159] by permission. © John Wiley & Sons, 2003.

Electron Transfer Dissociation (ETD)

- ET with anions formed in an external source (CI)

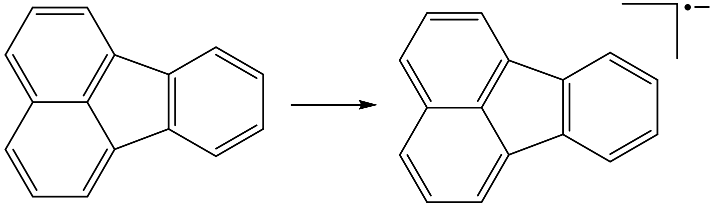

- Can be performed at larger pressures (also linear ion traps)
- Usually for doubly charged ions, triply charged ions react with large exothermicity
  → complete fragmentation

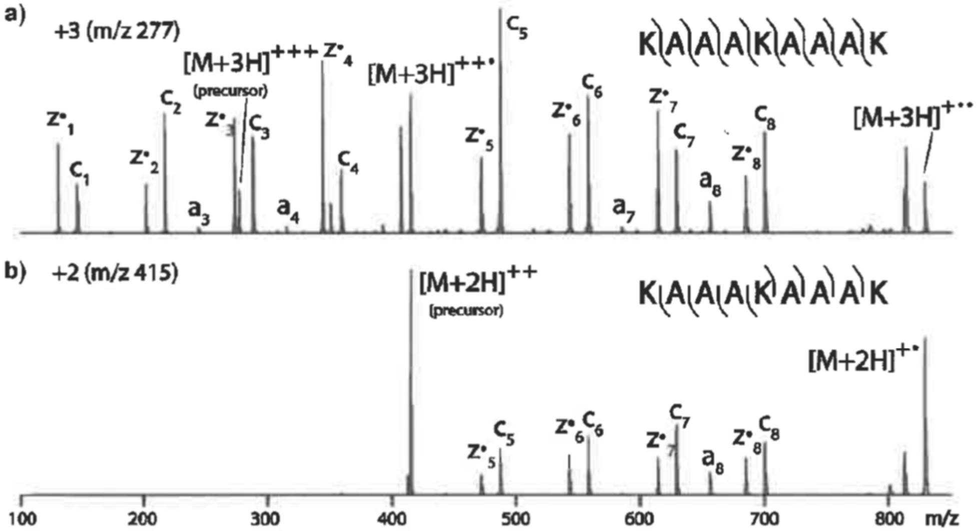

Fig. 9.40. Effect of precursor ion charge state on ETD product ion spectra of (**a**) the triply protonated peptide ion $[KAAAKAAAK+H]^{3+}$ and (**b**) the doubly protonated ion of the same peptide which only produces half of the possible *c*- and *z*-type fragments. Reproduced from Ref. [162] with permission. © American Chemical Society, 2007.

Surface-Induced Dissociation

- Usually for high-energy collision
- Often change-exchange processes
- Instrument adaption necessary

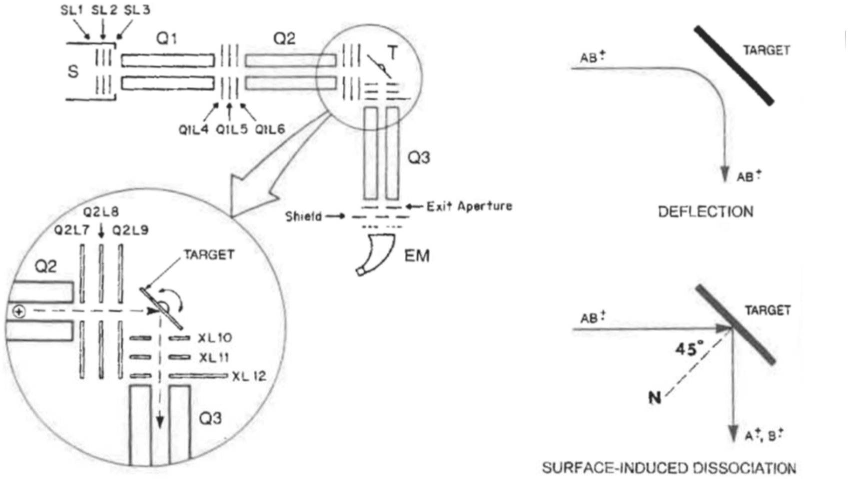

Fig. 9.9. Apparatus (*left*) and modes of operation (*right*) for SID with a modified triple quadrupole mass spectrometer. Reproduced from Ref. [34] with permission. © Elsevier Science, 1987.

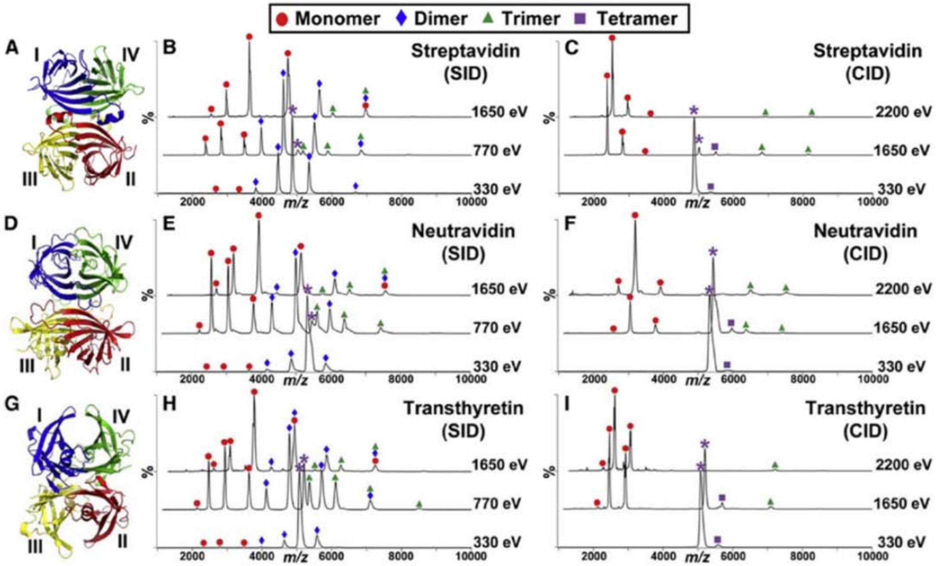

Nano-electrospray SID (middle panel) and CID (right panel) mass spectra of the charge-reduced +11 precursor of (B and C) SA, (E and F) neutravidin, and (H and I) TTR at three separate collision energies. All fragments are labeled based on their corresponding peaks detected in IM. The precursor ion in each spectrum is indicated by a purple asterisk. Crystal structures of (A) SA (PDB: 1SWB), (D) neutravidin (PDB: 1VYO), and (G) TTR (PDB: 1F41) are shown in the left panel. Subunits I, II, III, and IV are also shown in blue, green, yellow, and red, respectively. Reproduced from *Chemistry & Biology*, Vol. 22, Quintyn, Q., Yan, J., Wysocki, V.H., Surface-Induced Dissociation of Homotetramers with D2 Symmetry Yields their Assembly Pathways and Characterizes the Effect of Ligand Binding, pp. 583–592, Copyright (2015), (ref. 142) with permission from Elsevier.

analytical chemistry
Article
Cite This: *Anal. Chem.* 2018, 90, 7302−7309
pubs.acs.org/ac

Top-Down Deep Sequencing of Ubiquitin Using Two-Dimensional Mass Spectrometry

Federico Floris,[†] Lionel Chiron,[‡] Alice M. Lynch,[†] Mark P. Barrow,[†] Marc-André Delsuc,[‡,§]
and Peter B. O'Connor[*,†]

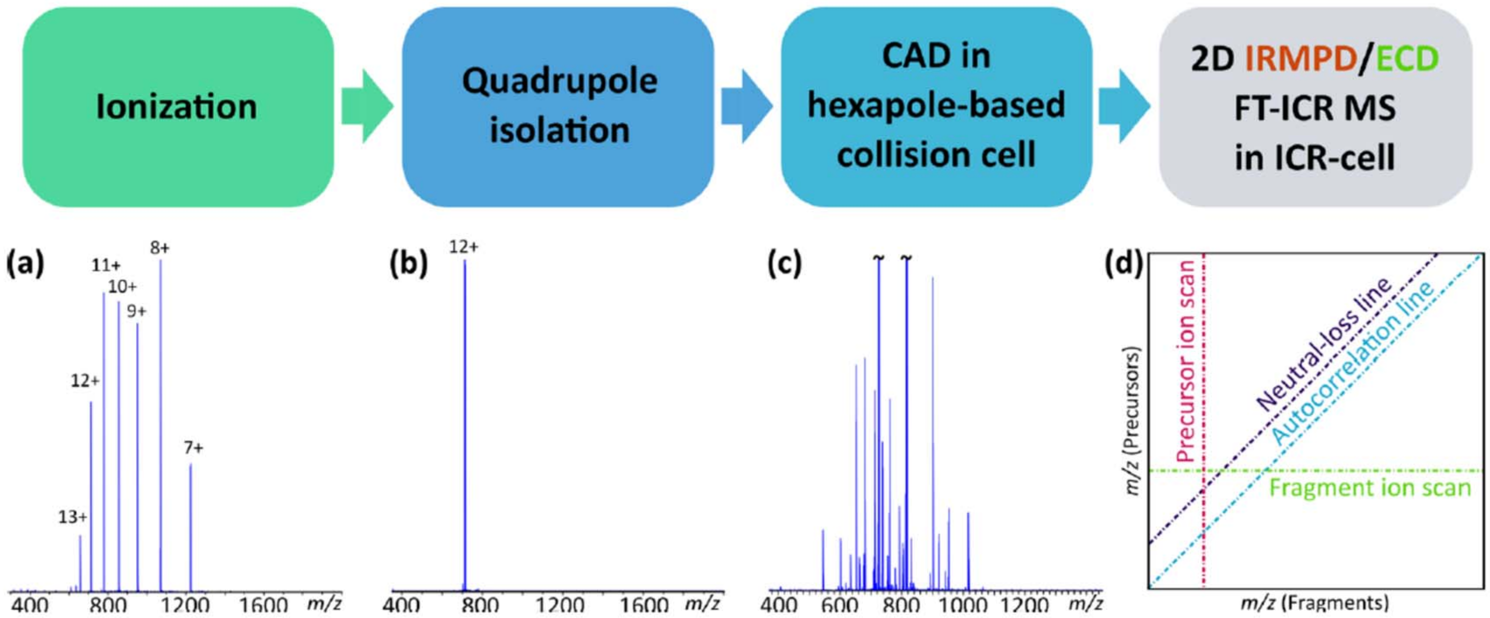

Figure 1. Workflow of MS/2DMS with representative spectra from the different steps of the procedure.

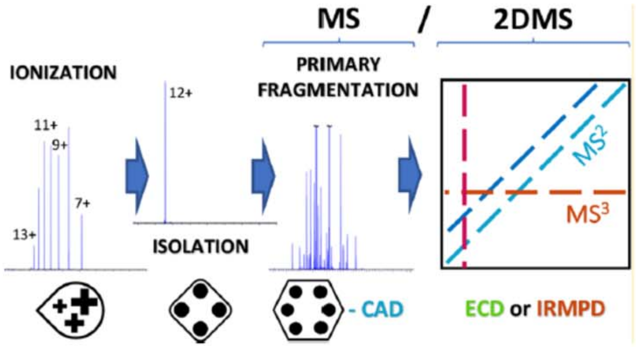

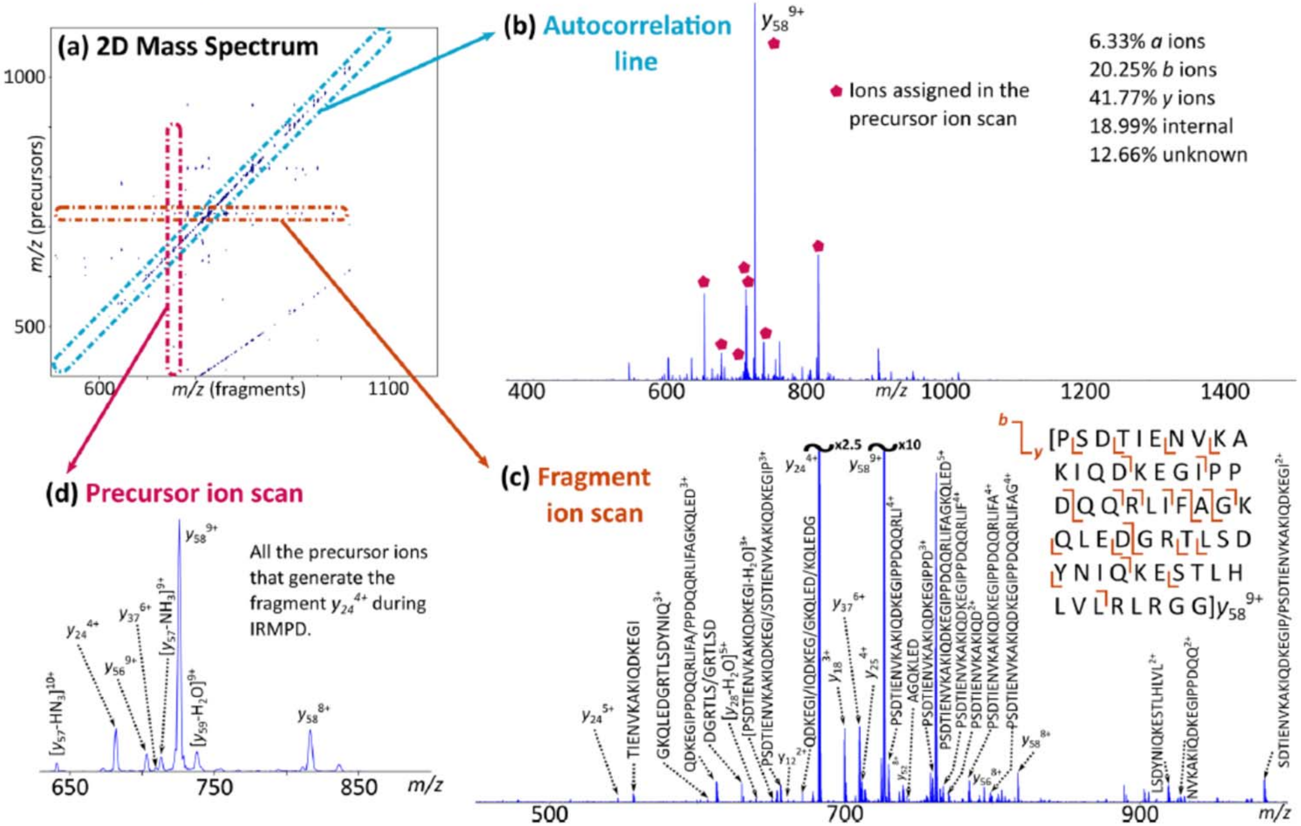

Figure 2. CAD-MS/IRMPD-2DMS of ubiquitin in denaturing conditions. (a) Two-dimensional mass spectrum, output of the CAD-MS/IRMPD-2DMS analysis of Ubi. The autocorrelation line and horizontal fragmentation patterns are observed. The curved line departing from the bottom of the spectrum constitutes harmonics signal. (b) Extraction of the autocorrelation line, with the percentages of the correctly assigned ions. Labeled ions represent the ions assigned through the precursor ion scan shown in spectrum d; they include ion $y_{58}{}^{9+}$, whose fragmentation pattern is shown in spectrum c. (c) Fragment ion scan of the ion $y_{58}{}^{9+}$ (m/z 726.2838) and respective cleavage coverage. Nondiagnostic neutral losses are not labeled for better visualization. (d) Precursor ion scan of the ion $y_{24}{}^{4+}$ (m/z 682.3820), constituting important information for the assignment of y ions on the autocorrelation line (b).

Conclusions

- MS/MS experiments → a unique tool to investigate structure of complex molecules
- Many variants of inducing fragmentation (CID, SID, IRMPD, ETD, ECD, and others)
- Useful for analysis of molecular ions (bond dissociation energies)